Progress In Electromagnetics Research, Vol. 129, 387–404, 2012

STUDY OF ELECTROMAGNETIC SCATTERING FROM SHIP WAKES ON PEC SEA SURFACES BY THE SMALL-SLOPE APPROXIMATION THEORY

R.-Q. Sun[1], M. Zhang[1, *], C. Wang[2], and Y. Chen[2]

[1]School of Science, Xidian University, Xi'an 710071, China

[2]Science and Technology on Electromagnetic Scattering Laboratory, Beijing 100854, China

Abstract—Electromagnetic (EM) scattering properties from the ship wakes on the two-dimensional (2-D) perfect electric conductor (PEC) sea surfaces are studied by utilizing the small-slope approximation (SSA) theory. Considering the limitations of using the ideal plane EM wave incident upon a rough sea surface of the limited size, the expressions of the scattered field and scattering amplitude are derived by utilizing the modified tapered incident field. Based on a simplified segmented ocean spectrum model, the bistatic and monostatic normalized radar cross sections (NRCS) from the PEC sea surfaces with and without ship wakes are calculated, respectively. Meanwhile, the variation of scattering coefficient as scattering angles is given and compared under different polarization states. The results show that the scattering from the PEC sea surfaces with ship wakes is evidently different from that without them in bistatic and monostatic scattering. This provides a basis to extract ship wake characteristics. Also it shows that the SSA is a very effective analysis method to deal with the EM scattering from the rough sea surface. Finally, the effect of different tapered factors on backscattering coefficient is discussed, and it is concluded that an artificial reflection from the boundaries and a scattering upwarping from low-grazing incidence can be avoided just when the tapered factor is relatively smaller. This gives the theoretical basis for the analysis of EM scattering characteristics of ship wakes on the PEC sea surface.

Received 14 April 2012, Accepted 18 June 2012, Scheduled 27 June 2012

* Corresponding author: Min Zhang (mzhang@mail.xidian.edu.cn).

1. INTRODUCTION

In recent years, with the continuous improvement of detection means, study of the domain of ocean remote sensing has attracted more and more attention from scholars. Ocean remote sensing plays an important role in wind speed inversion, ship parameters inversion by the wakes and synthetic aperture radar (SAR) imaging [1–3], etc. Its principle is mainly that, through airborne or spaceborne radar detection, the receiving power can be expressed by radar cross section of the radar equation [4–6]. The traditional airborne or spaceborne SAR imaging is based on the backscattering property of the sea surface. However, with the occurrence of bistatic and interferometric radar, it is necessary to research on the bistatic scattering characteristics of the sea surface. There are two major kinds of scattering theories of rough sea surfaces, i.e., numerical method and approximate method. As for numerical method, it has very high calculation precision, but its calculation is more complicated and hard to be realized. In this case, there is the necessity that study of approximate method be made. In the analysis of approximate theory, the more classical methods include Kirchhoff approximation (KA), small perturbation method (SPM) and two scale method (TSM) which combines KA and SPM [7–9]. Concerning KA, its basis is tangential plane approximation whose condition is that curvature radius of rough surface is much larger than incident wave length such that the hypothesis is hold that EM wave incident on an infinite plane is tangent to a point on rough surface. So KA method is appropriate to largescale rough surface, but cannot be applied to low grazing incidence. On the contrary, SPM is suitable for the micro-rough surface. Due to strict application scopes of these two methods based on statistical models of rough surfaces, there exist great limitations. TSM has extended the applied area of scattering of rough surfaces, but its disadvantage lies in that the concept of the cutoff wave number is introduced to distinguish between large-scale and small-scale rough surfaces when being calculated. The determination of the cutoff wave number is usually lack of scientific basis, Therefore, it is necessary to seek a theory that can accurately solve EM scattering of rough surfaces without regard to the structure of the rough surface. Bahar [10, 11] proposed the full wave method in early research for the theory mainly. In recent years, there appeared relevant numerical methods, such as the extended boundary condition method (EBCM), Monte Carlo (MC) and the finite difference of the time-domain (FDTD) method, and approximate method is mainly SSA [12–15]. Among them, the SSA method is an effective method of calculation applicable to any wavelength of the rough surface. And

it is a more precise approximate method by which the expressions of different orders derived are obtained by retaining the term numbers of the series expansions and can be degraded to the results of KA and SPM under certain conditions.

Some scholars apply the SSA method to the random sea surfaces with statistical significance and get the analytic expressions of the bistatic and backscattering coefficients related to statistical parameters such as correlation function including gauss type and exponential type, correlation length, root-mean-square height of the surface [16], etc. However, the sea surface usually studied is of the limited size. Statistical results are not affected by the choices of the different incident waves. In fact, the rough sea surface is truncated at the boundary [17]. This means that the surface current is forced to be zero outside the boundary. If there is an abrupt change of surface current from nonzero to zero, artificial reflection from the boundary will occur. Additionally, statistical results only roughly describe the EM characteristics of the rough sea surfaces, which does not satisfy the needs of the high resolution SAR imaging any more.

The paper adopts the SSA method to do research on the EM scattering properties of the ship wakes on the PEC sea surfaces from the viewpoint of the field. At the same time, the effects of the incident field on the scattering characteristics are fully considered in order to derive the corresponding calculation formulae of scattering amplitudes and obtain the relevant bistatic and backscattering coefficients. Finally, the results obtained are discussed and analyzed.

2. GEOMETRIC SIMULATION OF SEA SURFACES

The piecewise wave number spectrum is used to model 2-D sea surfaces. Concerning the marine remote sensing of SAR, in the case of moderate incident angles, the large-scale gravity wave spectrum is $S_1(k)$ and the small-scale capillary wave related to Bragg resonance is $S_2(k)$. Due to the dispersion characteristics of the sea waves, frequency spectrum differs from wave number spectrum, i.e., the long gravity wave and the short capillary wave have different non-linear dispersion relations and satisfy the relation $S(k) = S(\omega)d\omega/dk$, which fully shows that the changes from frequency domain to wave number domain are very complicated. So Fung and Lee use double wave number spectrum as the simplified form of Pierson-Moskowitz spectrum [18–21], i.e.,

$$S(k) = \begin{cases} S_1(k), & k < 0.04\,\text{rad/cm} \\ S_2(k), & k > 0.04\,\text{rad/cm} \end{cases} \tag{1}$$

To ensure the continuity of $S_1(k)$ and $S_2(k)$ at $k = 0.04\,\text{rad/cm}$,

the simplified piecewise wave number spectrum is given as follows:

$$S_1(k) = \frac{a}{k^3}\exp\left[-\frac{0.74g^2}{k^2u_{19.5}^4}\right] \tag{2}$$

$$S_2(k) = 0.875(2\pi)^{-1}\frac{g+3gk^2/13.177}{(gk+gk^3/13.177)^{(p+1)/2}} \tag{3}$$

where $g = 981\,\mathrm{cm/s^2}$, $a = 1.4\times10^{-3}$, $p = 5-\log_{10}u^*$, u^* is friction wind speed and larger than 12 cm/s, $u_{19.5}$ is the wind speed at the height of 19.5 m which is expressed as:

$$u_{19.5}=\frac{u^*}{0.4}\ln\frac{1950}{z_0}\,[\mathrm{cm/s}],\quad z_0=\frac{0.684}{u^*}+4.28\times10^{-5}u^{*^2}-0.0443\,[\mathrm{cm}] \tag{4}$$

In order to reflect the anisotropic features of sea spectrum caused by wind direction, the spreading function is usually introduced. This paper only adopts the spreading function of the cosine-squared type as follows:

$$G(\phi,\phi_0)=\begin{cases}2\cos^2(\phi-\phi_0)/\pi, & |\phi-\phi_0|<\pi/2\\ 0, & \pi/2\le|\phi-\phi_0|\le\pi\end{cases} \tag{5}$$

where ϕ_0 is the angle between wind direction and x-axis positive direction.

On the basis of 1-D sea spectrum and spreading function, 2-D sea spectrum can be written as $S(k,\phi)=S(k)G(\phi,\phi_0)$.

Simulation of sea surface is realized by using the statistical second-order approximation approaches mainly including the linear superposition method and the linear filter method. This paper uses the linear superposition method to model 2-D sea surfaces. Its principle is that to utilize hydrodynamics is to analyze and reveal dynamic properties and motion law of sea wave under a variety of situations. One of the most common models is Longuest-Higgins model which regards sea wave as stationary ergodic Gaussian random processes. And sea surface is the superposition of cosine signals with different amplitude, frequency and initial phase. Eventually, The wave height $z\,(x,\,y,\,t)$ of the 2-D time-varying sea surface can be expressed as:

$$z(x,y,t) = \sum_{i=1}^{M}\sum_{j=1}^{N}\sqrt{2S(\omega_i,\theta_j)\Delta\omega_i\Delta\theta_j}\cos[\omega_i t-k_i(x\cos\theta_j+y\sin\theta_j)+\varphi_{ij}] \tag{6}$$

where $S\,(\omega_i,\,\theta_j)$ is the 2-D sea spectrum, ω_i the uniform division point of the angle frequency, θ_j divided between $-\pi\sim\pi$ with the same interval, $\Delta\omega_i=\omega_{i+1}-\omega_i$ and $\Delta\theta_j=\theta_{j+1}-\theta_j$ the frequency and

angle differential element, respectively. The initial phase φ_{ij} uniformly distributes between $-\pi \sim \pi$, and k_i is wave number. As for the gravity wave, the dispersion relation is determined by gravity and its formula is $\omega_i = \sqrt{gk_i}$ where g is gravity acceleration and k_i is far less than 0.04 rad/cm. As for capillary wave, its dispersion relation is decided by surface tension and can be expressed as $\omega_i = \sqrt{\tau_s k_i^3/\rho}$ where τ_s [N/m] is sea surface tension, ρ [kg/m^3] is seawater density and τ_s/ρ is about 7.445×10^{-5} [m^3/s^2] at standard atmospheric pressure.

In this paper, the size of the simulated sea surface is 38.36×38.36 m, and there are 1024 sampling points at x and y directions, respectively. In this case, the sampling interval equals $\lambda_{inc}/8$ where λ_{inc} is the wavelength of the incident EM wave with 1 GHz frequency. The wind direction is 45°. The simulation result is shown in Figure 1.

3. GEOMETRIC SIMULATION OF MOVING SHIP WAKES

Ship wakes mainly include Kelvin wake and the turbulent wake which are two of the most important characteristics in target identification on the sea surface [22, 23]. The major research on ship wakes is to analyze the geometric simulation of Kelvin wakes which are the V-type wakes composed of the divergent and transverse waves when a ship is moving. The wave height distribution of Kelvin wakes has already had certain expressions beneficial to the study of all kinds of ships' sizes and velocities. However, the turbulent wakes [24] refer to the volume scattering of foam layers. So this paper only studies Kelvin wakes of ships.

While the wave elevation of Kelvin ship wake can be expressed by [25]

$$\varsigma(x,y) = \mathrm{Re} \int_{-\pi/2}^{\pi/2} A(\theta) \cdot \exp\left[k \sec^2\theta (ix\cos\theta + iy\sin\theta)\right] d\theta \tag{7}$$

where $k = g/V^2$, g is the acceleration of gravity, θ the angle between the wave direction and x axis, $A(\theta)$ the free spectrum that depicts the ship's characteristics, and its expression is

$$A(\theta) = \frac{4k}{V}\left(\sec^3\theta\right) H\left(k\sec^2\theta, \theta\right) \tag{8}$$

where $H(k, \theta)$ is Kochin function and can be written as

$$H(k,\theta) = \iint_{S_H} \sigma(x,y,z) \cdot \exp(k(ix\cos\theta + iy\sin\theta + z)) dS \tag{9}$$

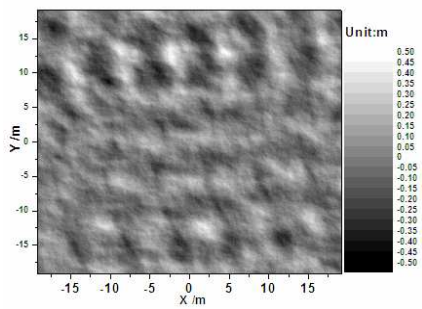

Figure 1. 2-D linear sea surface.

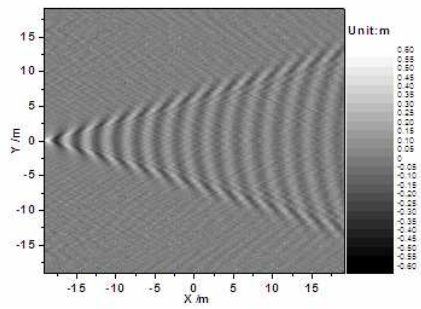

Figure 2. The geometric simulation of the Kelvin wake.

where S_H is the ship' s hull surface, and $\sigma(x, y, z)$ denotes the expression of the source strength, proportional to the local slope of the hull. Using the thin ship approximation, the ship' s hull is represented by a distribution of sources located on the longitudinal centreplane of the vessel. According to this theory, the source strengths are expressed as

$$\sigma(x, y, z) = -\frac{2V}{4\pi}\frac{\partial}{\partial x}f(x, z) \tag{10}$$

where f is the hull equation of the ship. If we consider a simple hull shape with parabolic waterlines, and if it is wall-sided with draft d, then

$$f(x, z) = \begin{cases} b(1 - x^2/l^2) & (-d < z < 0, -l < x < l) \\ 0 & (z < -d) \end{cases} \tag{11}$$

where b is the half-beam and l is the half-length of the ship.

In this paper, the size of the Kelvin wake simulated on calm sea surface is 38.36×38.36 m, and there are 1024 sampling points in x and y directions, respectively. Ship parameters are length 50 m, width 10 m, draft 2 m, and vessel speed 2 m/s. The simulation result is shown in Figure 2 above.

4. SCATTERING FIELD THEORY OF ROUGH SURFACE IN SSA

In SSA, the geometrical configuration adopted to resolve the wave-scattering problem from the 2-D randomly rough surface is given in Figure 3, where we consider a rough interface $z = h(\vec{r})$, with $\vec{r} = (x, y)$, between two homogenous half-spaces which are defined by their permittivity and permeability [26–28]. The time dependence

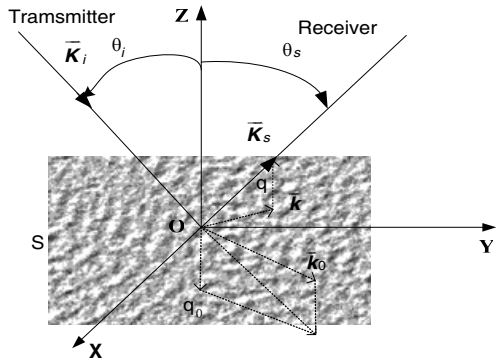

Figure 3. Geometry configuration for the wave scattering from 2-D surface.

is assumed to be $\exp(-i\omega t)$. And θ_i and θ_s are, respectively, incident and scattering elevation angles, and ϕ_i and ϕ_s are the incident and scattering azimuth angles, respectively. The incident wave vector can be expressed as $\vec{\mathbf{K}}_i = \vec{k}_0 - q_0\hat{z}$, where $\vec{k}_0$ and $-q_0$ are horizontal and vertical projections of the incident wave vector, respectively. The scattered wave vector is $\vec{\mathbf{K}}_s = +q\hat{z}$, where $\vec{k}$ and q are appropriate components of the scattered wave vector, respectively. q_0 and q can be expressed as [29, 30]:

$$q_0 = \sqrt{\omega^2/c^2 - k_0^2}, \quad q = \sqrt{\omega^2/c^2 - k^2}, \quad \mathrm{Im} q_0, q \geq 0 \tag{12}$$

In numerical simulations, the rough surface is of the limited size. This means that the surface current is forced to be zero for outside the rough surface. If there is an abrupt change of surface current from nonzero to zero, artificial reflection from the boundaries will occur. To avoid these problems, one way is to taper the incident wave so that the incident wave gradually decays to zero in a Gaussian manner for the place closed to the boundaries [31–36].

The unit vector in the direction of incidence is:

$$\hat{K}_i = \sin\theta_i\cos\phi_i\hat{x} + \sin\theta_i\sin\phi_i\hat{y} - \cos\theta_i\hat{z} \tag{13}$$

and the incident wave vector $\vec{K}_i = K_i\hat{K}_i = (\vec{k}_0, -q_0)$. The incident field can be expressed as:

$$\psi_{inc}\left(\vec{R}\right) = T\left(\vec{R}\right)\exp\left(-i\vec{k}_i\cdot\vec{R}\right) = \exp\left[i\left(\vec{K}_0\cdot\vec{r} - iq_0 z\right)(1+w)\right]\exp(-t)$$
$$= \exp[-iK_i(z\cos\theta_i - x\sin\theta_i\cos\phi_i - y\sin\theta_i\sin\phi_i)(1+w)]\exp(-t) \tag{14}$$

$$T\left(\vec{R}\right) = \exp\left[-i\left(\vec{K}_i\cdot\vec{R}\right)w\right]\exp(-t) \tag{15}$$

where $\vec{R} = (\vec{r}, q_0) = (x, y, z)$, $t = t_x + t_y$, and

$$t_x = \frac{(x\cos\theta_i\cos\phi_i + ycos\theta_i\sin\phi_i + z\sin\theta_i)^2}{g^2\cos^2\theta_i} \tag{16}$$

$$t_y = \frac{(-x\sin\phi_i + ycos\phi_i)^2}{g^2} \tag{17}$$

$$w = \frac{1}{K_i^2}\left(\frac{2t_x - 1}{g^2\cos^2\theta_i} + \frac{2t_y - 1}{g^2}\right) \tag{18}$$

and ψ_{inc} is electric field E or magnetic field H depending on the polarization, and g is the parameter that controls the tapering of the incident wave.

The unit vector in the direction of scattering is:

$$\hat{K}_s = \sin\theta_s\cos\phi_s\hat{x} + \sin\theta_s\sin\phi_s\hat{y} + \cos\theta_s\hat{z} \tag{19}$$

and the scattered wave vector is $\vec{K}_s = K_s\hat{K}_s = (\vec{k}, q)$. The scattered field can be expressed as:

$$\psi_{sc}(x, y, z) = q^{1/2}\int \exp\left(i\vec{k}\cdot\vec{r} + iqz\right)\bar{\bar{S}}\left(\vec{k}, \vec{k}_0\right)d\vec{k} \tag{20}$$

Taking into account the far-field approximation, the scattering amplitude matrix corresponding to first-order SSA (SSA1) can be modified as

$$\bar{\bar{S}}\left(\vec{k}, \vec{k}_0\right) = \frac{2(qq_0)^{1/2}}{\sqrt{P_{inc}}\,(q+q_0)}\bar{\bar{B}}\left(\vec{k}, \vec{k}_0\right) \times\int T\left(\vec{R}\right)\exp\left[-i\left(\vec{k}-\vec{k}_0\right)\cdot\vec{r}+i(q+q_0)h\left(\vec{r}\right)\right]d\vec{r}\,\frac{1}{(2\pi)^2} \tag{21}$$

where $\vec{r}$ is the projecting component in the x-y plane of spatial location vector $\vec{R}$, and P_{inc} is the incident wave power received by the rough surface and can be expressed as:

$$P_{inc} = \iint |\psi_{inc}(x, y, 0)|^2 dxdy \tag{22}$$

and $\bar{\bar{S}} = \begin{bmatrix} S_{11} & S_{12} \\ S_{21} & S_{22} \end{bmatrix}$, $\bar{\bar{B}} = \begin{bmatrix} B_{11} & B_{12} \\ B_{21} & B_{22} \end{bmatrix}$ where subscripts "1" and "2" represent the vertical and horizontal polarization, respectively. The left hand number represents the polarization mode of the receiving antenna, and the right hand number represents that of the transmitting antenna. For the sake of convenience this paper only deals with co-polarizations HH and VV.

Suppose that the second layer be a perfect conductor where the EM field can not penetrate. Assuming the permittivity in the second medium tends to infinity, we find that Bragg's kernel matrix $\bar{\bar{B}}\left(\vec{k}, \vec{k}_0\right)$ can be expressed as:

$$B_{11}\left(\vec{k}, \vec{k}_0\right) = \frac{K_s^2\left(\vec{k} \cdot \vec{k}_0\right) - k^2 k_0^2}{q_k^{(1)} q_{k_0}^{(1)} k k_0}, \quad B_{22}\left(\vec{k}, \vec{k}_0\right) = -\frac{\vec{k} \cdot \vec{k}_0}{k k_0} \tag{23}$$

We choose medium 1 as air and medium 2 as PEC sea surface, i.e., the boundary is the interface between air and PEC sea surface. This means that the complex relative permittivity of the air is $\varepsilon_1 = (1, 0)$. $-q_{k_0}^{(1)}$ and $q_k^{(1)}$ are the vertical components of the incident wave vector in the air and the scattered wave vector in the sea, respectively. They can be expressed as:

$$q_k^{(1)} = \sqrt{\varepsilon_1 \frac{\omega^2}{c^2} - k^2}, \quad q_{k_0}^{(1)} = \sqrt{\varepsilon_1 \frac{\omega^2}{c^2} - k_0^2}, \quad \mathrm{Im} q_k^{(1)}, q_{k_0}^{(1)} \geq 0 \tag{24}$$

which is the same to the Equation (12).

In terms of rough surface scattering amplitudes calculated by SSA1, the NRCS can be obtained by

$$\sigma_{pq}^0 = 4\pi q q_0 \Delta S_{pq}\left(\vec{k}, \vec{k}_0\right)\left(\Delta S_{pq}\left(\vec{k}, \vec{k}_0\right)\right)^* \tag{25}$$

where

$$\Delta S_{pq}\left(\vec{k}, \vec{k}_0\right) = S_{pq}\left(\vec{k}, \vec{k}_0\right) - \left\langle S_{pq}\left(\vec{k}, \vec{k}_0\right)\right\rangle \tag{26}$$

The expression (25) represents the scattered field corresponding to single rough surface, and subscript pq denotes polarization state. Due to the random characteristics of the sea surface, the final bistatic NRCS and the backscattering coefficient are calculated as an average, i.e.,

$$\overline{\sigma_{pq}^0} = \left\langle \sigma_{pq}^0 \right\rangle \tag{27}$$

Each NRCS is obtained over 100 realizations of sea surfaces.

5. NUMERICAL RESULTS AND ANALYSIS

As for the simulations of bistatic NRCS and backscattering coefficients, sea surface parameters are: the size of the sea surface is $L_x = L_y = 38.36$ m sampled with 1024 points in each direction, and the speed wind at 19.5 m is 5 m/s and its direction 45°. Ship wake parameters are: its size the same as that of sea surface, ship length 50 m, ship width 10 m, draft 2 m, and ship speed 2 m/s. EM parameters are: the frequency

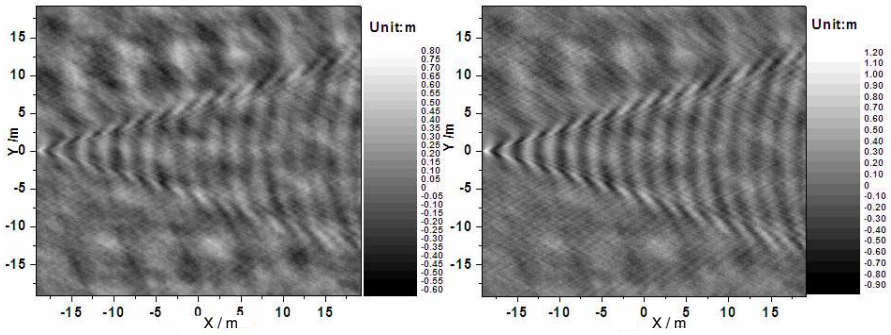

Figure 4. Linear superposition of linear sea surface and ship wake. (a) and (b) denote that the superposition ratios of the sea surface and the ship wake are 1 to1 and 1 to 2, respectively.

1 GHz, the incident angles 0° and 60°, the tapering parameter g chosen to be $L_x/4$, and the average NRCS obtained over 100 realizations of sea surfaces.

5.1. Linear Superposition of Linear Sea Surface and Ship Wake

The linear sea surface and the ship wake are given in Figures 1 and 2, respectively. To analyze EM scattering characteristics of ship wake on the PEC sea surface, for convenience, we utilize the linear superposition of linear sea surface and ship wake, which can be shown in Figure 4, where (a) and (b) denote that the superposition ratios of the sea surface and the ship wake are 1 to 1 and 1 to 2, respectively.

5.2. Comparing of Bistatic NRCS

Figure 5 shows bistatic NRCS results of Figure 1. (a) and (b) represent incident angles of 0° and 60°, respectively. In Figures 6 and 7, the bistatic NRCS results corresponding to Figures 4(a) and 4(b) respectively are given and co-polarization comparisons between the sea surface with the ship wake and that without ship wakes are also made. At the same time, the average bistatic NRCS results are given in Figures 8 and 9.

From these figures, it is seen that in the vicinity of specular direction, the average NRCS from single sea surface is significantly larger than that of the sea surface with ship wakes. And with the increase of ship wake proportion, the average NRCS of the sea surface

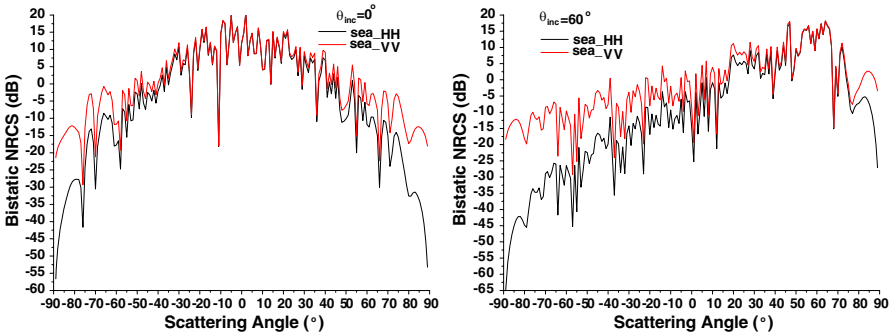

Figure 5. Bistatic NRCS results of Figure 1. (a) and (b) denote incident angles of 0° and 60°, respectively, where black line is HH polarization and red line is VV polarization.

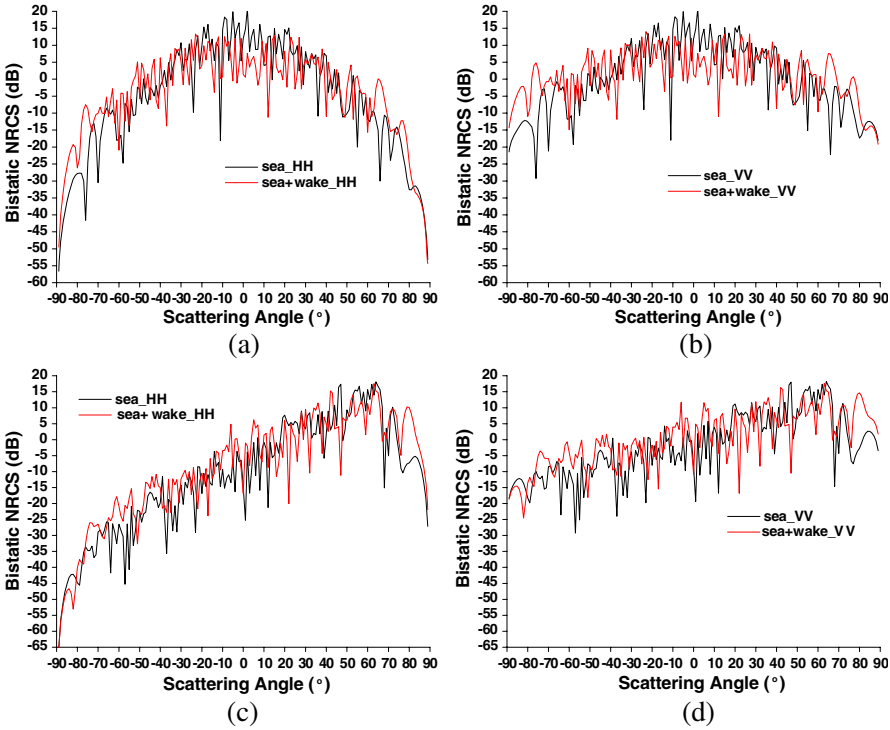

Figure 6. Co-polarization comparisons between bistatic NRCS results of Figure 4(a) (red line) and that of Figure 1 (black line). (a) and (b) are corresponding to incident angle of 0°, and (c) and (d) are corresponding to incident angle of 60°.

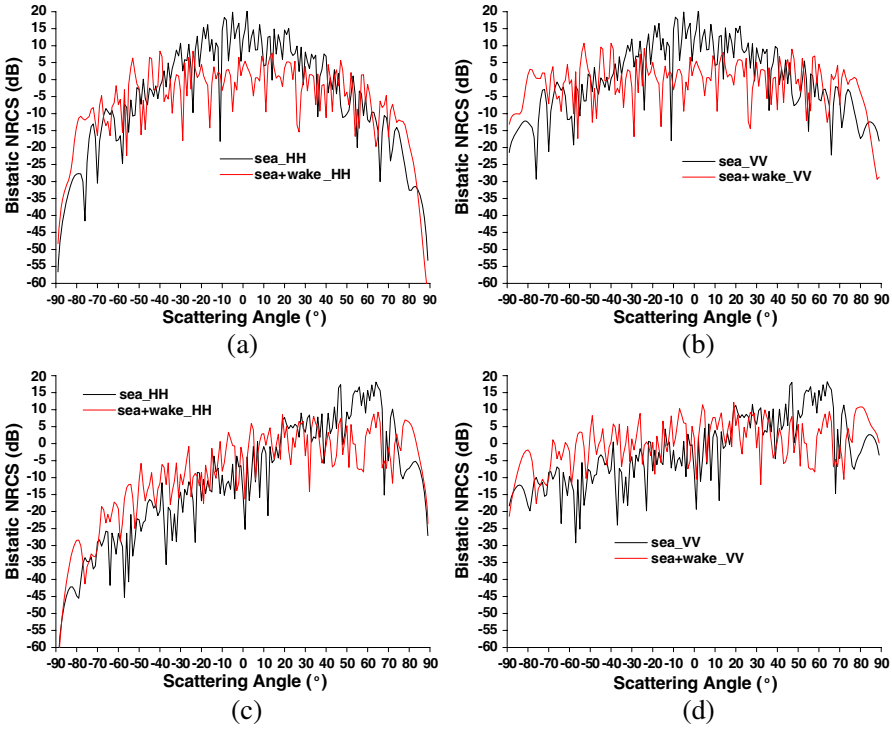

Figure 7. Co-polarization comparisons between bistatic NRCS results of Figure 4(b) (red line) and that of Figure 1 (black line). (a) and (b) are corresponding to incident angle of 0°, and (c) and (d) are corresponding to incident angle of 60°.

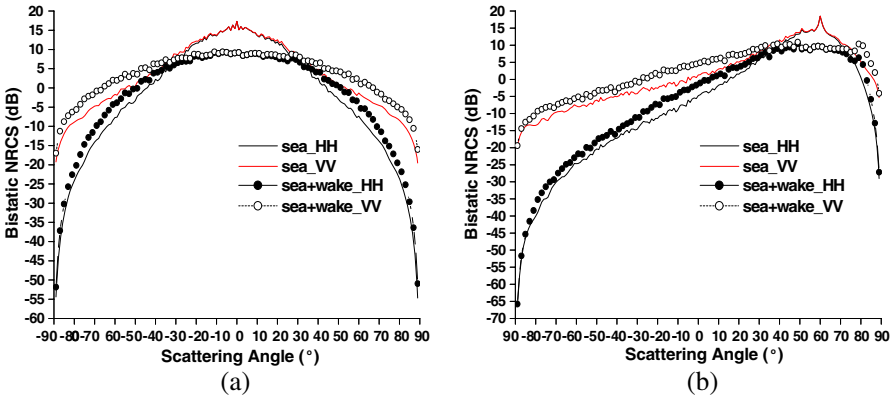

Figure 8. Average bistatic NRCS results corresponding to Figure 6.

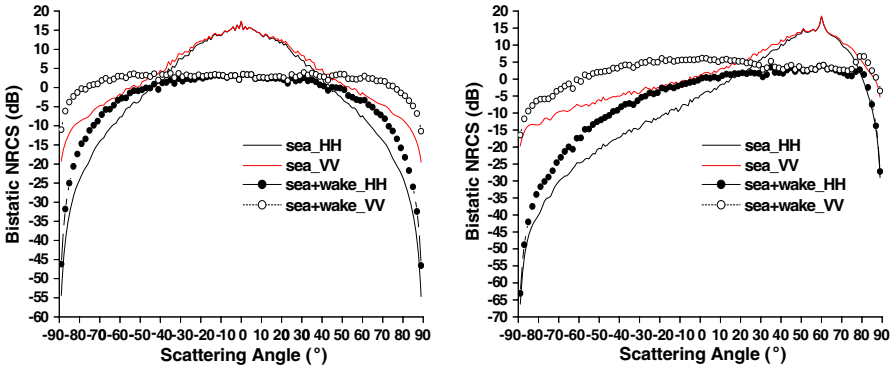

Figure 9. Average bistatic NRCS results corresponding to Figure 7.

with ship wakes becomes much smaller. On the contrary, As the scattering angles gradually departing from the specular regions, the average NRCS from the sea surface with ship wakes is evidently greater than that of single sea surface. What's more, we find the larger ship wakes proportion is, the difference between single sea surface and that with ship wakes becomes more obvious except the grazing incidence.

5.3. Comparing of Backscattering Coefficients

5.3.1. Average Backscattering Coefficients

In what follows, we put emphasis on the backscattering case, i.e., $\theta_s = \theta_i$, $\varphi_i = 0°$, $\varphi_s = 180°$. The average backscattering coefficients versus incident angles for the same simulation parameters are shown in Figure 10. From this figure, it is seen that in the quasi-specular region, the backscattering coefficients of single sea surface are evidently larger than that of the sea surface with ship wakes. However, as the incident angle increases, the coefficient for the sea surface with ship wakes is larger than that of single sea surface. As mentioned above, the difference of the backscattering coefficients between single sea surface and that with ship wakes becomes great.

5.3.2. Effect of Tapered Factor on Backscattering Coefficient

Due to the use of the modified tapered incident wave, where tapered factor g is major parameter controlling incident wave. Herein, we only discuss the influence of different tapered factors on backscattering coefficients calculated from Figure 1, which is shown in Figure 11.

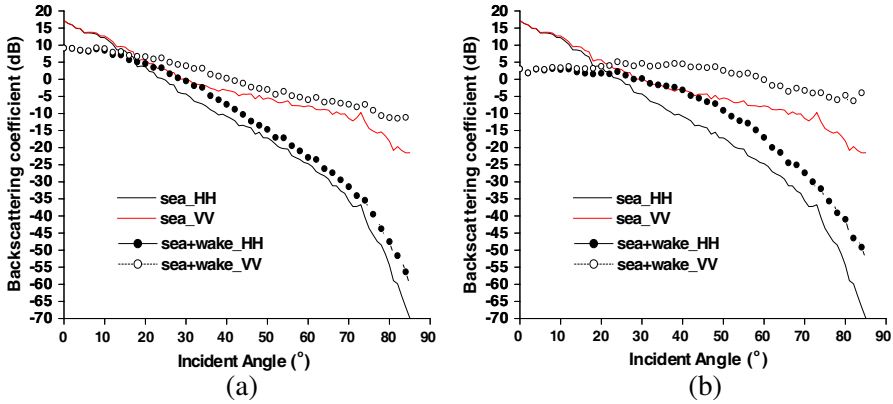

Figure 10. Average backscattering coefficients versus angles.

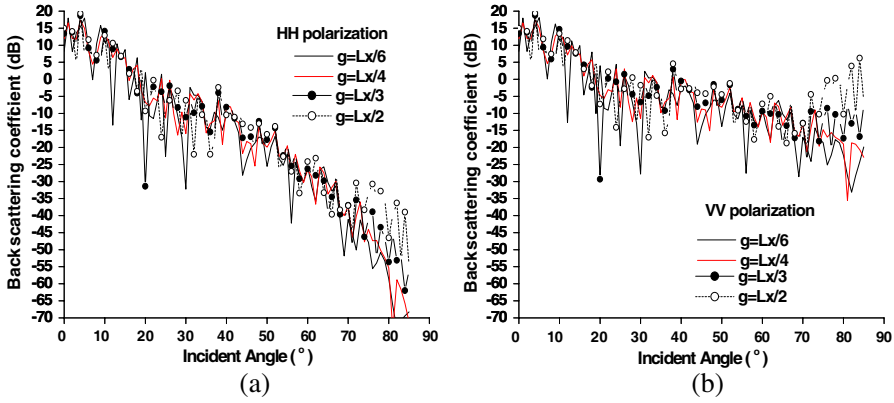

Figure 11. Effects of different tapered factors on backscattering coefficients calculated from Figure 1. (a) HH polarization. (b) VV polarization.

Among them, (a) and (b) show that, in the quasi-specular region, different tapered factors hardly affect the scattering results, but with the incident angles increasing, the scattering intensity become large correspondingly. Especially in VV polarization, the larger the tapered factors are, the more easily the upwarping scattering results occur. It leads to the occurrence of artificial reflection at the boundaries. Meanwhile, it is now clear why some literature chooses tapered factor between $L_x/10$ and $L_x/4$. However, accurate choice of tapered factor mainly depends on the experimental data.

6. CONCLUSION

In this paper, based on 2-D linear sea surface and Kelvin wake of a ship, the SSA technique has been applied to calculate the scattering from 2-D PEC sea surfaces for both with ship wakes and without them. This method bridges the gap between the two classical approaches: SPM and KA. It should be valid for arbitrary roughness having small slopes, irrespective of the wavelength of the radiation. SSA is also used in either deterministic or statistical cases which are often encountered in practice and is of obvious interest. In addition, taking into account the limitations of using the ideal plane incident wave on the rough sea surface of the limited size, the expressions of the scattered field and scattering amplitude are derived by utilizing the modified tapered incident wave. A comparative study has been made to the distinct features of both bistatic NRCS and backscattering coefficient due to linear superposition of linear sea surface and ship wake. What's more, from the numerical results of bistatic NRCS and the backscattering coefficient, it is seen that the scattering signals of the PEC sea surface with ship wake are distinguished from that of single PEC sea surface, and their difference exceeds 10 dB at part scattering or incident angles. It is concluded that the scattering features of the PEC sea surface with ship wake are helpful to the recognition and parameter inversion of the ship wake.

ACKNOWLEDGMENT

The authors would like to thank the Fundamental Research Funds for the Central Universities, the National Natural Science Foundation of China under Grant No. 60871070 and the Foundation of the National Electromagnetic Scattering Laboratory to support this kind of research.

REFERENCES

1. Baussard, A., M. Rochdi, and A. Khenchaf, "PO/mec-based scattering model for complex objects on a sea surface," *Progress In Electromagnetics Research*, Vol. 111, 229–251, 2011.
2. Ai, J., X. Qi, W. Yu, et al., "A novel ship wake CFAR detection algorithm based on SCR enhancement and normalized hough transform," *IEEE Trans. on Geosci. Remote Sens.*, Vol. 8, No. 4, 681–685, 2011.

3. Zhao, Y. W., M. Zhang, X. Geng, and P. Zhou, "A comprehensive facet model for bistatic SAR imagery of dynamic ocean scene," *Progress In Electromagnetics Research*, Vol. 123, 427–445, 2012.
4. Valenzuela, G. R., "Theories for the interaction of electromagnetic and oceanic waves — A review," *Boundary Layer Meteorology*, Vol. 13, 61–85, 1978.
5. Jin, Y. Q. and Z. X. Li, "Numerical simulation of radar surveillance for the ship target and oceanic clutters in two-dimensional model," *Radio Science*, Vol. 38, No. 3, 1045, 2003.
6. Chen, H., M. Zhang, and H.-C. Yin, "Faced-based treatment on microwave bistatic scattering of three-dimensional sea surface with electrically large ship," *Progress In Electromagnetics Research*, Vol. 123, 385–405, 2012.
7. Thorsos, E. I., "The validity of the Kirchhoff approximation for rough surface scattering using a Gaussian roughness spectrum," *J. Acoust. Soc. Am.*, Vol. 83, No. 1, 78–92, 1988.
8. Guo. L.-X., Y. Liang, J. Li, and Z.-S. Wu, "A high order intergral SPM for the conducting rough surface scattering with the tapered wave incidence-TE case," *Progress In Electromagnetics Research*, Vol. 114, 333–352, 2011.
9. Lee, P. H. Y., et al., "Wind-speed dependence of small-grazing-angle microwave backscatter from sea surfaces," *IEEE Trans. on Antennas and Propagat.*, Vol. 44, No. 3, 333–340, 1996.
10. Bahar, E. and B. S. Lee, "Full wave solutions for rough-surface bistatic radar cross sections: Comparison with small perturbation, physical optics, numerical and experimental results," *Radio Science*, Vol. 29, No. 2, 407–429, 1994.
11. Bahar, E. and B. S. Lee, "Radar scatter cross section for two-dimensional random rough surfaces-full wave solutions and comparisons with experiments," *Wave in Radom Media*, Vol. 6, 1–23, 1996.
12. Vaitilingom, L. and A. Khenchaf, "Radar cross sections of sea and ground clutter estimated by two scale model and small slope approximation in HF-VHF bands," *Progress In Electromagnetics Research B*, Vol. 29, 311–338, 2011.
13. Voronovich, A. G., "Small-slope approximation in wave scattering by rough surfaces," *Sov. Phys. JETP*, Vol. 62, 65–70, 1985.
14. Berginc, G. and C. Bourrely, "The small-slope approximation method applied to a three-dimensional slab with rough boundaries," *Progress In Electromagnetics Research*, Vol. 73, 131–211, 2007.

15. Toporkov, J. V. and G. S. Brown, "Numerical study of the extended Kirchhoff approach and the lowest order small slope approximation for scattering from ocean-like surfaces: Doppler analysis," *IEEE Trans. on Antennas and Propagat.*, Vol. 50, No. 4, 417–425, Apr. 2002.
16. Chevalier, B. and G. Berginc, "Small-slope approximation method: scattering of a vector wave from 2D dielectric and metallic surfaces with Gaussian and non-Gaussian statistics," *Proceedings of SPIE*, Vol. 4100, 22–32, 2000.
17. Tsang, L. and J. A. Kong, *Scattering of Electromagnetic Waves, Advanced Topics*, Wiley Series in Remote Sensing, Wiley Interscience, New York, 2001.
18. Fung, A. K. and K. K. Lee, "A semi-empirical sea-spectrum model for scattering coefficient estimation," *IEEE Journal of Oceanic Engineering*, Vol. 7, 166–176, 1982.
19. Qi, C., Z. Zhao, W. Yang, Z.-P. Nie, and G. Chen, "Electromagnetic scattering and doppler analysis of three-dimensional breaking wave crests at low-grazing angles," *Progress In Electromagnetics Research*, Vol. 119, 239–252, 2011.
20. Pierson, W. J. and L. Moscowitz, "A proposed spectral form for fully developed wind seas based on the similarity theory of S. A. Kitaigorodskii," *J. Geophys. Res.*, Vol. 69, No. 24, 5181–5190, 1964.
21. Yang, W., Z. Zhao, C. Qi, W. Liu, and Z.-P. Nie, "Iterative hybrid method for electromagnetic scattering from a 3-D object above a 2-D random dielectric rough surface," *Progress In Electromagnetics Research*, Vol. 117, 435–448, 2011.
22. Shakeri, M., M. Tavakolinejad, and J. H. Duncan, "An experimental investigation of divergent bow waves simulated by a two-dimensional plus temporal wave marker technique," *J. Fluid Mech.*, Vol. 634, 217–243, 2009.
23. Hennings, R. R., W. Alpers, and A. Viola, "Radar imaging of Kelvin arms of ship wakes," *Int. J. Remote Sensing*, Vol. 20, No. 13, 2519–2543, 1999.
24. Milgram, J. H., R. A. Skop, R. D. Pelter, and O. M. Griffin, "Modeling short sea wave energy distributions in the far wakes of ships," *J. Geophys. Res.*, Vol. 98, No. C4, 7115–7124. 1993.
25. Sun, R. Q., G. Luo, M. Zhang, and C. Wang, "Electromagnetic scattering model of the Kelvin wake and turbulent wake by a moving ship," *Waves in Random Media*, Vol. 21, No. 3, 501–504, 2011.

26. Mcdaniel, S. T., "An extension of the small-slope approximation for rough surface scattering," *Waves in Random Media*, Vol. 5, No. 2, 201–214, 1995.
27. Albert, M. D., Y. J. Lee, H.-T. Ewe, and H.-T. Chuah, "Multilayer model formulation and analysis of radar backscattering from sea ice," *Progress In Electromagnetics Research*, Vol. 128, 267–290, 2012.
28. Voronovich, A. G. and V. U. Zavorotny, "Theoretical model for scattering of radar signals in Ku- and C-bands from a rough sea surface with breaking waves," *Waves in Random Media*, Vol. 11, No. 3, 247–269, 2001.
29. Zhang, M., W. Luo, G. Luo, C. Wang, and H.-C. Yin, "Composite scattering of ship on sea surface with breaking waves," *Progress In Electromagnetics Research*, Vol. 123, 263–277, 2012.
30. Voronovich, A. G., "Small-slope approximation for electromagnetic wave scattering at a rough interface of two dielectric half-spaces," *Waves in Random Media*, Vol. 4, 337–367, 1994.
31. Li, X. F. and X. J. Xu, "Scattering and doppler spectral analysis for two-dimensional linear and nonlinear sea surfaces," *IEEE Trans. on Geosci. Remote Sens.*, Vol. 49, No. 2, 603–611, 2011.
32. Berginc, G., "Small-slope approximation method: A further study of vector wave scattering from two-dimensional surfaces and comparison with experimental data," *Progress In Electromagnetics Research*, Vol. 37, 251–287, 2002.
33. Ji, W.-J. and C.-M. Tong, "Bistatic scattering from two-dimensional dielectric ocean rough surface with a PEC object partially embedded by using the G-SMCG method," *Progress In Electromagnetics Research*, Vol. 105, 119–139, 2010.
34. Tsang, L., J. A. Kong, K. H. Ding, and C. A. Ao, *Scattering of Electromagnetic Waves, Numerical Simulations*, 270–271, Wiley Series in Remote Sensing, Wiley Interscience, New York, 2001.
35. Ye, H. and Y. Jin, "Parameterization of the tapered incidence wave for numerical simulation of electromagnetic scattering from rough surfaces," *IEEE Trans. on Antennas and Propagat.*, Vol. 53, No. 3, 1234–1237, 2005.
36. Toporkov, J. V., R. S. Awadallah, and G. S. Brown, "Issues related to the use of Gaussian-like incident field for low grazing angle scattering," *J. of the Opt. Soc. Amer. A, Opt. Image Sci. and Vision*, Vol. 16, No. 1, 176–187, 1999.